Macromolecules

Article

pubs.acs.org/Macromolecules

Component-Specific Heterogeneity and Differential Phase Partitioning in Gradient Copolymers Revealed by Solids NMR

Andrew Clough, Jessica L. Sigle, Arifuzzaman Tapash, Lance Gill, Nitin V. Patil, Joe Zhou, and Jeffery L. White*

Department of Chemistry, Oklahoma State University, Stillwater, Oklahoma 74078, United States

ABSTRACT: Gradient copolymers can exhibit physical properties that are different than their block polymer analogues. Property variations should depend upon differences in the molecular arrangement of individual comonomers in the polymer chain and in the gradient zone of each chain as well as the morphological arrangement of those chains in space. Here we describe experimental approaches based on fast and slow magic-angle spinning (MAS) NMR, which reveal the amount of rigid and soft phases in styrene–butadiene gradient copolymers with component specific resolution. In addition, we introduce a spin-counting strategy that quantitatively and directly determines the amount of the low-T_g, or "soft", butadiene component that is incorporated into the rigid domains and also the amount of high-T_g, or "hard", styrene component that is incorporated into the mobile domains. In total, the experiments provide bulk rigidity, amount of polybutadiene partitioned in both soft and hard phases and the amount of polystyrene partitioned in each phase. We show that the synthesis conditions can be changed to vary the partitioning of each gradient copolymer component in a systematic way and propose that the interphase between the hard and soft domains is responsible for differential partitioning.

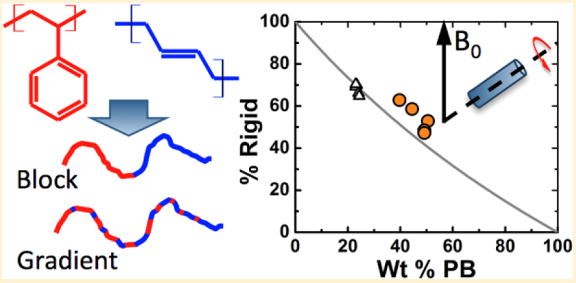

INTRODUCTION

Controlled polymerization methods can create a vast array of new materials, as exemplified by the recent development of gradient copolymers, in which the individual comonomer concentrations vary across the length of any particular chain.[1−6] While recent advances in controlled living polymerization techniques have led to many new gradient copolymers (linear, parabolic, hyperbolic, etc.), *direct experimental evidence* about how gradient copolymers organize or order, the temperature dependence of that ordering, and the relationship between morphology and chain architecture is difficult to assess, especially for solid systems. What is clear from the investigations published to date is that gradient copolymers are complex, heterogeneous systems characterized by distributions in glass transitions, chain dynamics, and relaxation times that can reflect the type of gradient that predominately exists in the polymer chains.[7−10] In contrast to block copolymers, interfaces are often "blurred" and poorly defined. In solution, their micellar properties are also different than typical block copolymers.[11,12] New experimental strategies that can assess, with chain specificity, the type and breadth of morphological structural heterogeneity in gradient copolymers are necessary for improved material properties.

Like many well-known copolymer systems, gradient copolymers often contain monomers that in pure form would generate polymers with large glass transition temperature (T_g) differences. Such differences are attractive for end-use materials, since strength and flexibility are optimized over very wide temperature ranges, and this is one reason why the styrene–butadiene gradient systems are so attractive. Therefore, one could generally expect that a quantitative measure of the fraction of rigid versus soft chains in the overall gradient copolymer morphology would constitute a relevant parameter, given its direct relationship to high versus low-T_g character. In principle, bulk rigid versus soft fractions in heterogeneous copolymers can be determined via traditional static ^{1}H NMR echo methods based on fits of the free-induction decays or echoes, as has effectively been employed by the Saalwaechter group and extended to cases involving relatively inexpensive low-field or benchtop NMR systems.[13−15] Some technical issues make it difficult to exactly determine the total signal intensity at the initial condition, due to very fast dipolar relaxation during the receiver recovery period, but ways to minimize this problem are known and discussed in the literature involving different solid echo and dipolar refocusing pulse sequences.[14,20] The presence of such small absolute, but consistent, errors in the total initial signal amplitude does not preclude the use of these methods for meaningful polymer structure/property investigations.

A key disadvantage of applying static solid-state NMR methods to mixed polymeric systems is that component-specific responses are often difficult or impossible to discern. Stated differently, the chemical component contribution to the soft or hard phase cannot easily be identified in a mixed

Received: January 27, 2014
Revised: March 28, 2014
Published: April 8, 2014

   dx.doi.org/10.1021/ma500213k | *Macromolecules* 2014, 47, 2625−2631

polymer system by static methods. Such complications are compounded in gradient copolymer systems, compared to simple block polymers, as differential monomer incorporation leads to unique and complex gradient shapes at the comonomer interfaces, and most likely, these complex interfaces influence the final morphology.

In this contribution, experimental strategies using magic-angle spinning (MAS) solid-state NMR are applied to styrene–butadiene (PS–PB) gradient copolymers synthesized under different conditions in order to identify and quantify the amount of rigid and mobile phases in the copolymers. We investigate an approach based on comparisons between fast and slow MAS ^{1}H experiments as a first step toward determination of component-specific behaviors in rigid and mobile segments of the gradient copolymers. In addition, we introduce a spin-counting strategy, adapted from our previous contribution related to catalyst characterizations,[16] that easily quantifies the amount of the low-T_g, or "soft", butadiene component that is incorporated into the rigid domains of gradient copolymers. We demonstrate that the fast MAS and spin-counting NMR methods can detect, in an experimentally straightforward approach, differential properties of the copolymers that are modified by varying the gradient copolymer synthesis conditions. The key advantage of the spin-counting approach is the ability to compare measured signal intensities for each polymer component to the theoretical intensities based on known compositions. Our work follows and builds upon previous work by the Saalwaechter group, which described in detail how magnetic resonance methods at low and high field could be used to address differential behavior in copolymers and to detect "hardening" and "softening" of different phases.[13−15] Other experimental approaches that exploit NMR's unique advantages for detecting differential mobility in complex polymer systems are available and typically rely on relaxation (primarily T_2 or $T_{1\rho}$) or specific magnetic interactions (e.g., dipolar, chemical shift anisotropy) to determine structure–property relationships. Interested readers may wish to consult representative texts, review articles, and recent examples as described in refs 17 and 18.

EXPERIMENTAL SECTION

Solid-state MAS and fast-MAS NMR measurements were collected on a Bruker DSX-300 spectrometer operating at a magnetic field strength of 7.05 T, using a 2.0 mm double-resonance magic-angle spinning probe provided by Revolution NMR in Fort Collins, CO. Measurements were recorded using a windowless eight-count composite 90° pulse sequence for background suppression,[21] with a typical pulse width of 2.1 μs, a receiver dead time of 3–4 μs, and a 10 s repetition delay time (longer than $5T_{1H}$ for either PS or PB). ^{1}H spin-counting measurements were acquired at 5 kHz, using a Bruker 4.0 mm MAS probe on the same spectrometer. Spectra were obtained using a single 90° pulse with a 3.5 μs pulse width and a 10 s repetition delay time. Approximately 2 mg of polydimethylsiloxane (PDMS) was added to rotors containing known masses of polymer, as described in detail in our previous work.[16] As communicated in that report, Teflon spacers were used to limit the sample region to the middle ca. 20% volume element of the rotor to ensure maximum rf homogeneity, thereby resulting in uniform excitation and determination of the intensity per ^{1}H using the PDMS internal standard. The effective sample region in the rotor was a cylinder of 4 mm in diameter and ca. 4 mm in length. Control experiments, in which a known amount of hexamethylbenzene (HMB) and a known amount of PDMS were added to the rotor, yielded 101 ± 4% of the expected theoretical HMB intensity.

All block copolymers were prepared by batch living anionic polymerization in cyclohexane similar to the method described by Leibler and co-workers.[19] The first block is a pure polybutadiene block, followed by copolymerization of equal weights of styrene and butadiene and then finished with additional styrene to increase the molecular weights of styrene blocks. The discrete block copolymer would skip the copolymerization step with an adjustment in butadiene and styrene at first and last block to maintain similar molecular weight. The gradient copolymer denoted as PS-grad-PB was prepared in the absence of any polar modifiers, while the PS-grad-PB_THF sample was done with addition of tetrahydrofuran (THF) at a molar ratio of THF/Li = 2.6 before alkyllithium was added. The pure PS was a low melt flow index, commercial general purposed polystyrene by free radical bulk polymerization. In contrast, the pure polybutadiene copolymer was a commercial medium vinyl high molecular weight polybutadiene by anionic polymerization.

High-resolution ^{1}H solution NMR revealed that the composition of the PS–PB block copolymer was 51:49 wt:wt % styrene:butadiene. Solution NMR revealed that the two gradient copolymers described above contained 49–51 wt % butadiene, essentially identical to the PS–PB block copolymer. Two additional gradient copolymers, prepared in the same manner as the PS-grad-PB_THF, had additional styrene added to the end block to provide samples with modified content but with the same gradient structure. These two materials are denoted as grad_THFb and grad_THFc in Tables 1 and 2.

RESULTS AND DISCUSSION

Figure 1 shows representative ^{1}H MAS NMR spectra for a 51:49 wt:wt % styrene–butadiene (PS–PB) block copolymer

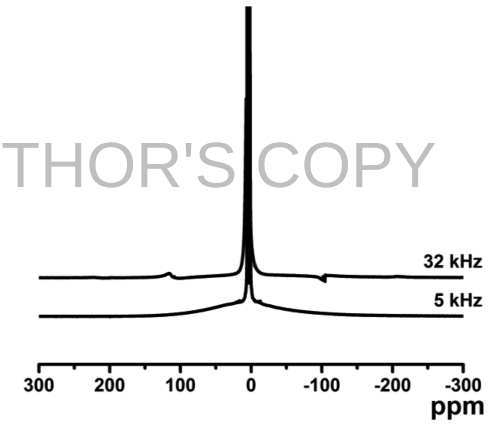

Figure 1. ^{1}H MAS NMR and fast MAS spectra for a PS–PB block copolymer obtained at spinning speeds of 5 and 32 kHz, respectively.

obtained at MAS spinning speeds of 5 and 32 kHz. As is expected for a styrene–butadiene copolymer in the solid state, two types of signals are observed at 5 kHz MAS, including a narrow set of signals near 0 ppm and an extremely broad ca. 200 ppm (60 kHz) signal extending across the majority of the spectral window. This broad signal arises from rigid polystyrene segments whose motional correlation times are too slow to average homonuclear ^{1}H dipolar couplings. As the spinning speed is increased to 32 kHz, the broad component is essentially eliminated, resolving into the aromatic and aliphatic PS peaks. Spectra acquired at 32 kHz should, within the known constraints of signal loss due to receiver dead time, reflect the total signal arising from all polymer segments. In addition, errors in total signal intensity that may arise from fitting of broad components due to small errors in the baseline selection are removed at 32 kHz.

A simple two-component rigid and mobile (hard and soft) model is used here to analyze the spectra, even though more complex analyses should be possible in future investigations.

dx.doi.org/10.1021/ma500213k | Macromolecules 2014, 47, 2625–2631

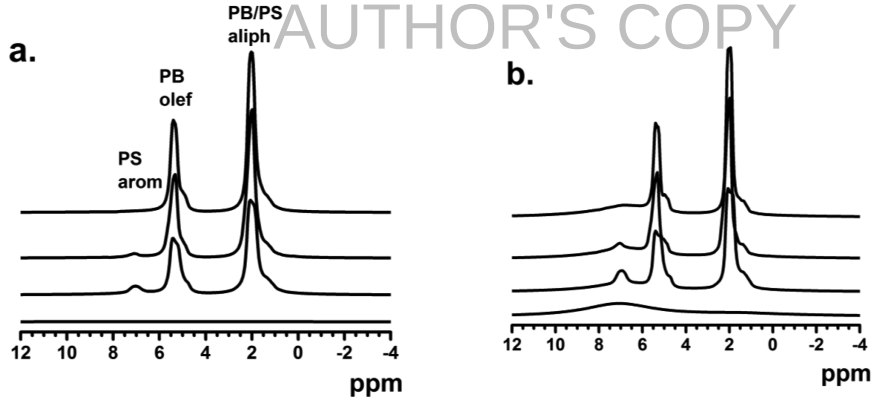

Figure 2. From bottom to top: ^{1}H MAS NMR spectra of pure PS, PS-grad-PB_THF, PS-grad-PB (no THF), and the PS−PB block copolymer at (a) 5 kHz and (b) 32 kHz. All spectra were acquired at room temperature.

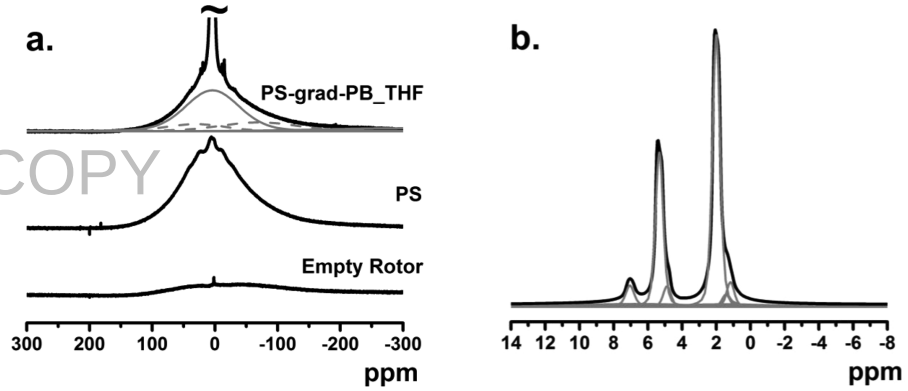

Figure 3. (a) ^{1}H MAS NMR spectra for the empty rotor, pure PS, and PS-grad-PB_THF at 5 kHz. The dashed line in the upper spectrum denotes the background contribution, and the gray line is the rigid PS contribution. Additional contributions corresponding to a narrower, but still rigid, PS component and its sidebands are included in the deconvolution but are too small to show in this figure. (b) Isotropic region of the ^{1}H MAS NMR spectra for the PS-grad-PB_THF copolymer, with the gray lines indicating the individual components used to fit the line shape. The two smaller PB components near 1 and 5 ppm arise from 1,2-enchainments.

Mobile components are defined as narrow signals whose line widths at half-maximum are less than 2 ppm in spectra obtained at 5 kHz MAS. Expansion of the isotropic region is shown in Figures 2a and 2b for the two gradient copolymers denoted as PS-grad-PB_THF and PS-grad-PB and the same PS−PB block copolymer previously shown in Figure 1. As all copolymers are essentially identical near 50:50 wt:wt % styrene:butadiene composition, variations in the individual peaks in the room temperature spectra of Figure 2 reflect differences in the chain dynamics of the individual components. For reference, the spectrum for pure PS is shown as the bottom trace in both Figures 2a and 2b, revealing that in the isotropic region of the ^{1}H MAS spectrum the PS is uniform at 5 kHz but exhibits the expected aromatic:aliphatic ratio at 32 kHz (albeit with broad signals relative to the mobile components of the copolymers). In Figure 2a, relatively narrow PS aromatic signals are observed only for the two gradient copolymer samples (middle traces), while narrow PB olefinic and aliphatic signals are observed in all copolymers. The narrow gradient copolymer PS signals become more visible at 32 kHz (Figure 2b), while the PB signals are much less sensitive to increased MAS speeds, albeit for slightly better resolution of minor signals arising from 1,2-butadiene and cis enchainments. At 32 kHz, a PS aromatic signal is detected for the PS−PB block copolymer (top trace in Figure 2b), similar to that observed for pure PS. Qualitatively, the different aromatic signal widths for PS in the gradient copolymers (middle traces in Figure 2a) relative to pure PS and a control PS−PB block copolymer of similar composition indicate that some PS chain segments get incorporated in more mobile regions and that the amount of PS in such an environment may be altered by addition of a Lewis base modifier like THF.

The total integrated area of any narrow liquid-like signals appearing in the isotropic chemical shift region of spectra acquired at 5 kHz represents the amount of mobile or soft-phase chains present in any copolymer sample. As discussed previously, spectra acquired at 32 kHz should reflect the total signal intensity. A comparison of the total integrated area of all signals acquired at 32 kHz to the intensity of the mobile segment signals at 5 kHz, including spinning sidebands, provides a quantitative definition for the bulk percent rigidity of the sample, corresponding to the percent of ^{1}H signal from the rigid components. The following simple relationship is used to define bulk rigid fraction in these materials based on slow versus fast MAS data:

$$\text{bulk \% rigid} = [(I_{32} - I_5^{M})/I_{32}] \times 100 \quad (1)$$

where I_{32} represents the total intensity at 32 kHz and I_5^{M} denotes only the mobile intensity (sum of all narrow signals) in the 5 kHz spectrum. Intensities were obtained by deconvoluting the spectra using a set of Voigt line shapes to fit both the mobile and broad components of the spectra, as shown in

dx.doi.org/10.1021/ma500213k | Macromolecules 2014, 47, 2625−2631

Figure 3. A broad but reproducible background signal arising from the stator rotor is obtained at each spinning speed, as shown in Figure 3a, and is easily subtracted out from each spectrum during the deconvolution process. Using acquisition conditions described in the Experimental Section, the total overall intensity detected in the 5 kHz spectrum is routinely equal to 97−99% of the total intensity detected in the 32 kHz spectrum. For reference, pure atactic PS (T_g = 100 °C) exhibits no narrow peak at 5 kHz, while the % rigidity in pure PB (T_g = −95 °C) was at most 2% using this method. *Within the error of the experiment, the expected result of completely rigid and completely soft is obtained for pure PS and pure PB, respectively.*

In order to assess the fast/slow MAS NMR method for determination of the percent rigid fraction in gradient copolymers, measurements were made on the PS−PB block copolymer and four gradient copolymers, the results of which are given in Table 1. Comparison of the last three samples, where the preparation of the gradient interface is identical but the wt % PS is varied, indicates that increasing the hard segment PS content leads to the expected increase in bulk % rigid fraction. The PS−PB block copolymer, PS-grad-PB, and PS-grad-PB_THF, which have similar wt % PB but different interfacial structures, have very similar bulk % rigid fraction. Previous published work on some commercial styrene−butadiene copolymers using static NMR methods yielded bulk rigid fractions near 70%, but in those cases, the butadiene content was much lower at 22−25 wt %.[14]

Table 1. Measured Fast/Slow MAS NMR Results for ^{1}H Bulk Percent Rigid Fraction in the Block and Gradient Copolymers[a]

sample	wt % PS	mol % PS	^{1}H % PS	^{1}H % rigid
block	50.8	34.9	41.7	36.9
PS-grad-PB	50.8	34.9	41.7	35.0
PS-grad-PB_THF	49.5	33.7	40.4	38.4
grad_THFb	55.5	39.3	46.3	44.7
grad_THFc	60.3	44.1	51.3	49.3

[a]The last two samples were prepared similar to PS-grad-PB_THF, but with additional styrene monomer feed at the end of the polymerization process. The amount of PS in each copolymer was determined by solution ^{1}H NMR measurements.

The fastest reliable spinning speed in our laboratory is 32 kHz, which explains the choice of this seemingly arbitrary MAS speed. The working assumption for defining "fast" is that the homogeneous dipolar couplings are rendered heterogeneous via spinning, and the broad dipolar line width for strongly coupled protons will be converted to an isotropic spectrum with accompanying sidebands. Figure 1 shows that this occurs with 32 kHz MAS for PS−PB copolymers. The preference would be to spin even faster, e.g. 50 kHz, and as more laboratories have access to even faster MAS equipment, this will become routinely accessible. Typical MAS conditions for routine solids experiments are in the "slow" 4−7 kHz range, so 5 kHz was chosen as representative of standard conditions. More importantly, it is well-known that narrow line widths, on the order of the 2 ppm criteria for defining "mobile" or liquid-like resolution discussed later, are only obtained in solid macromolecules when significant isotropic motion is present. The slow MAS data are only used to get the mobile fraction intensity, and this will be the same at any common slow speed; the sample is the primary source of spatial averaging, not the MAS. Therefore, given that all intensity is taken from the fast MAS data, whether that is 30 or 32 or 40 kHz, and *only* the mobile intensity is taken from the slow data, the results should be invariant to minor deviations in the spinning speeds used as long as the criteria described above are satisfied.

The differential MAS spinning speed method described above quickly and easily yields the percent rigidity for any polymer or copolymer. In addition, it is amenable to variable-temperature data collection so that one can determine how the bulk rigidity changes over temperature ranges relevant to end-use applications. However, the real advantage relative to other methods lies in the ability to get component specific information. For example, the appearance of mobile PS in the gradient copolymers is readily observed in the spectra. One could determine the area of the narrow PS signals in the 5 kHz spectra of Figure 1 or 2 and compare that intensity to the total PS signal, yielding the percent of PS that is mobile. This is simply not possible using traditional static wide-line methods. However, fitting the broad rigid PS at low spinning speeds is more difficult than fitting narrow components, and additional error may be introduced. More importantly, the possibility of rigid PB chains, whose signals are harder to discern than the appearance of a mobile PS peak, would lead to an over-estimation of the total PS signal. Further, frictional heating effects at fast MAS speeds could complicate the ability to get accurate difference signals, as the sample temperature is effectively higher relative to the slow MAS condition unless cooling air is applied and controlled (vide infra). This method is attractive due to its simplicity, and the possibility for complete automation, but in this initial study, the need for a complementary validation method exists.

Therefore, an improved determination of the amount of mobile PS and rigid PB can be accomplished in a straightforward manner by employing a quantitative spin-counting internal calibration technique, which makes use of PDMS as an internal standard. PDMS is an attractive standard as it provides a very sharp liquid-like signal at 0.2 ppm, well outside of the spectral region of interest, as evident in Figure 4.

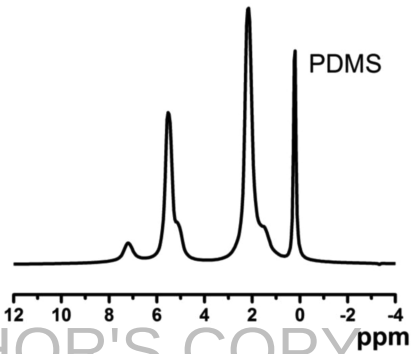

Figure 4. The 5 kHz ^{1}H MAS NMR spin-counting spectrum of the PS-grad-PB_THF sample previously described above. The narrow signal at 0.2 ppm is from the PDMS spin-counting standard.

A known amount of PDMS is added to a known amount of copolymer sample, and both are centralized in the rotor via top and bottom Teflon spacers, to minimize radio frequency field inhomogeneity.[16] Control experiments done using pure HMB, a plastic organic crystal whose static line width is intermediate between that of PS and PB, verifies the confidence of this method by generating yields of 101 ± 4% of the expected

dx.doi.org/10.1021/ma500213k | *Macromolecules* 2014, 47, 2625−2631

theoretical HMB intensity. Comparison of the total integrated intensity of the PDMS signal with measured PDMS mass allows one to determine the intensity per ^{1}H in the spectra. This provides a means to compare observed signal intensities to expected values based on measured sample mass.

Based on the composition of the copolymers derived from solution NMR and the measured sample mass, the expected signal intensity per ^{1}H of the PS and PB components is known. As a test, the total observed PB signal of a pure PB sample was measured, giving 102.3% of the expected mobile signal. The higher than expected signal is attributed to the measured intensity in the PDMS peak, which is the largest source of uncertainty in this method. In order to minimize the amount of error, the signal intensities were measured by numerical integration rather than by manual peak fitting techniques. Because of the overlap of the aliphatic PS and PB signals, only the mobile aromatic PS and olefinic PB signals were considered in the calculations to determine the amount of mobile PS and rigid PB, respectively. To provide a more accurate representation of the rigid PB fraction, the 1,2-PB contribution to the PB determined from solution NMR was used to obtain the number of olefinic ^{1}H per unit mass. Non-negligible amounts of 1,2-PB were observed, with ∼10% in the block copolymer and PS-grad-PB and ∼15% in PS-grad-PB_THF series.

Results of spin-counting measurements performed on the block copolymer, PS-grad-PB, PS-grad-PB_THF, and the grad_THFb and THFc samples are presented in Table 2. The percent of PS in a mobile phase was found by comparing the intensity in the mobile aromatic PS peak to the total expected aromatic PS intensity based on the sample mass, wt % PS, and intensity per ^{1}H determined by the PDMS standard. Consistent with the observations from the slow and fast MAS measurements depicted in Figure 2, the block copolymer is found to contain almost no mobile PS (0.5%), while 8.1% of the PS in PS-grad-PB_THF is mobile. The fraction of rigid PB, whose existence is not easily discerned from simply looking at the spectra, is accounted for by examining the percentage of mobile olefinic PB intensity missing from the expected olefinic intensity. A similar trend to that observed for mobile PS is observed, with the block copolymer having the least rigid PB (8.7%), while PS-grad-PB_THF exhibits the largest fraction of PB in a rigid phase (24.5%). *Taken together, these data indicate a heterogeneous distribution of local segmental environments for the gradient materials, the extent of which can be varied based on the synthesis conditions.* These results provide quantitative and component-specific evidence for the concept of "PS-softening" and "PB-hardening". In addition, the results for the grad_THFb and grad_THFc copolymers (last two columns of Table 2) show the same phase complexity as the PS-grad-PB_THF material, but with a slightly larger rigid PB fraction and a slightly smaller mobile PS fraction. This result, along with the increased total percent rigidity, is completely consistent with what is expected for appending a larger PS block in the same synthesis used to make the PS-grad-PB_THF copolymer.

Since PB accounts for about 60% of the ^{1}H intensity in these 50:50 wt:wt % copolymers, the amount of rigid PB and mobile PS observed by spin-counting MAS would indicate that we should have a net increase in the bulk rigid fraction, in contrast to the fast MAS results shown previously in Table 1 and reproduced in the last row of Table 2. In order to understand this discrepancy, the bulk rigid fraction is calculated directly from the spin-counting measurements by replacing the intensity at 32 kHz in eq 1 with the total expected signal intensity as determined from the mass of the copolymer samples. The total missing signal is measured to be less than 5% of the expected signal, which is consistent with the small (∼1−3%) differences observed between the total intensities at 5 and 32 kHz noted earlier. As shown in Table 2, the bulk rigid fraction is increased to 48−63% for the four copolymers via the absolute spin-counting method, with all of the gradient copolymers exceeding the block copolymer. While there is a noticeable difference in the bulk rigid fraction measured by the spin-counting versus the fast/slow MAS methods, it appears to be a systematic effect and does not affect any comparison between samples if the same method of determining bulk rigid fraction is used. The reason for the difference is still being studied but is believed to be due to difficulties in correctly phasing the empty rotor background of the 2.0 mm fast MAS, which in turn could lead to a systematic error in the measured total intensity by that method and temperature effects in the sample caused by the frictional heating at 32 kHz. Control experiments on our system show that the frictional heating effect is the largest source of error in the fast MAS method, since our fast MAS probe does not have active variable-temperature control capability. Chemical shift thermometry using standard lead nitrate experiments reveals a 50 K difference in sample temperature at 32 kHz versus 5 kHz in our probe, resulting in a measurable but reproducible decrease in total signal intensity at 32 kHz due to thermal population differences. Under active temperature control of the sample, this source of error will be eliminated, and this method should provide quantitative accuracy comparable to the spin-counting approach described below. In contrast, the spin-counting method is internally calibrated, relies only upon a single spectral acquisition, and its absolute accuracy clearly makes it the gold standard. The key advantage of the spin-counting method compared to the fast MAS approach is that all information can be obtained using standard MAS probes and that difference measurements are not required in order to determine rigid phase contents. However, the fast/slow MAS method is attractive due to its simplicity and potential for

Table 2. Summary of Fast/Slow ^{1}H MAS Percent Rigid Measurements and Spin-Counting NMR Measurements for the PS−PB Block Copolymer and the Two PS-grad-PB Samples of Similar Butadiene wt %[a]

sample	block	PS-grad-PB	PS-grad-PB_THF	grad_THFb	grad_THFc
modifier	no THF	no THF	THF	THF	THF
wt % PS	50.8	50.8	49.5	55.5	60.3
^{1}H % PS	41.7	41.7	40.4	46.3	51.3
% 1,2-PB	9.8	9.7	14.9	13.3	13.1
% mobile PS (spin count)	0.5	2.8	8.1	7.5	6.1
% rigid PB (spin count)	8.7	13.4	24.5	26.5	26.8
% missing signal (spin count)	−1.1	4.1	4.2	−3.2	−5.7
^{1}H % rigid total	47.2	48.3	52.9	58.6	62.8
^{1}H % rigid total (fast MAS)	36.9	35.0	38.4	44.7	49.3

[a]The weight percent values and percent of PB that is 1,2 PB (% 1,2 PB) reported were obtained by ^{1}H solution NMR. Note that the last two columns, denoted THF_b and THF_c, are the same gradient preparation used for PS-grad-PB_THF, but with an additional PS block appended, hence the overall higher total percent rigid fraction.

dx.doi.org/10.1021/ma500213k | *Macromolecules* 2014, 47, 2625−2631

complete automation, and for this reason we report it here and will work to continue to improve its absolute accuracy.

A graph of our data, along with these prior results, is given in Figure 5. A curved line corresponding to the expected bulk % rigid fraction in the case of no mixing of rigid and mobile components (i.e., PS is completely rigid and PB is completely mobile) is included in order to provide a point of reference; the curve is not a straight line due to the different proton contents in styrene and butadiene. As shown in Figure 5, all three of the gradient copolymers prepared with the THF modifier lie signficantly above the predicted line, while the block copolymer is only 2% above the theoretical percent rigid value but below the non-THF gradient copolymer.

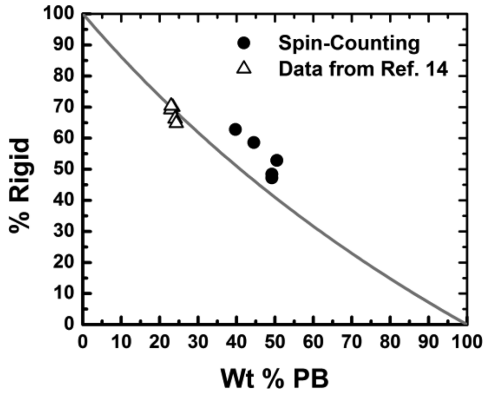

Figure 5. Comparison of bulk percent rigid fraction for styrene–butadiene copolymers versus weight percent butadiene content for materials used in this study (filled symbols analyzed by spin-counting), and prior results from ref 14 (open symbols).

As specified in the beginning of this work, we have chosen a simple two-phase model in which the appearance of narrow isotropic line shapes at 5 kHz defines a component as mobile. While not shown here, narrow peaks for the mobile components at other commonly used slow MAS speeds, e.g., 3–10 kHz, are essentially identical to those obtained at 5 kHz, as the line shapes for the mobile components are determined by the rapid reorientation of those chains and not MAS. We do not attempt to assign any directly observed signals to interfacial components, i.e., to analyze the direct spectral data in the spin-counting or fast/slow MAS approach using a three-phase (or higher) model. While this is a logical extension for future work, the value in the experimental approach described here is that the simple and robust spin-counting experiment can quickly identify gradient copolymers whose soft PS and hard PB phase amounts indicate deviation from block copolymer behavior. We would certainly expect that gradient copolymers, compared to traditional block copolymers, would have a more complex distribution of relevant relaxation times (e.g., T_2) or dynamics (e.g., dipolar or CSA modulation) and that those distributions could affect final mechanical properties. However, the process for tailoring chain interfaces begins with synthesis, and the ability to determine in a straightforward experiment how changes in synthesis, like varying modifier type or amount, impacts where the "low-T_g" and "high-T_g" monomer units ultimately reside in the material is critical. The spin-counting results described above clearly show that the amount of rigid PB and the amount of soft PS in the THF modified gradient copolymers *exceeds* that expected for block copolymers, and to our knowledge, this component specific chain information cannot be duplicated using any previously described experimental approach. In this way, one can quickly determine which synthesis schemes show the most promise for making high-gradient materials and identify which products are worthy of additional experimental evaluation. Future work will focus on using variable temperature methods to extract central correlation time constants and their distributions, which should accurately reflect differential interfacial dynamics in gradient copolymers relative to their block copolymer analogues.

CONCLUSIONS

A novel experimental approach is described that quantitatively reveals the amount of rigid and soft phases in styrene–butadiene gradient copolymers with component specific resolution and proves that differential phase partitioning takes place in gradient copolymers that does not occur in similar block copolymers. We introduce a spin-counting strategy that accurately determines the amount of the low-T_g, or "soft", butadiene component that is incorporated into the rigid domains of gradient copolymers and simultaneously reveals how much of the high-T_g, or "hard", styrene component is incorporated into the soft phase. Most importantly, we demonstrate that the polymer distributions can be manipulated by varying the gradient copolymer synthesis conditions and that these component specific distributions change even when the overall chemical composition of the system is constant. Future work will focus on predicting the component-specific hard/soft phase distributions based on the choice and amount of modifier used in the synthesis, investigating the temperature-dependence of the component specific morphological distributions, and investigating the structure of the interface.

AUTHOR INFORMATION

Corresponding Author

*E-mail jeff.white@okstate.edu (J.L.W.)

Present Address

J.Z.: Chevron Phillips Chemical Company LP.

Notes

The authors declare no competing financial interest.

ACKNOWLEDGMENTS

The authors gratefully acknowledge the National Science Foundation (GOALI grant DMR-1203848) and Chevron Phillips Chemical Company LP for support of this work.

REFERENCES

(1) Beginn, U. Gradient Copolymers. *Colloid Polym. Sci.* **2008**, *286*, 1465.

(2) Wang, J. S.; Matyjaszewski, K. Controlled Living Radical Polymerization: Halogen Atom Transfer Radical Polymerization. *Macromolecules* **1995**, *28*, 7901.

(3) Jakubowski, W.; Juhari, A.; Best, A.; Koynov, K.; Pakula, T.; Matyjaaszewski, K. Comparison of Thermomechanical Properties of Statistical, Gradient, and Block Copolymers of Isobornyl Acrylate and n-Butyl Acrylate. *Polymer* **2008**, *49*, 1567.

(4) Gallow, K.; Jhoun, Y.; Tang, W.; Genzer, J.; Loo, Y.-L. Cloud Point Suppression in Dilute Solutions of Model Gradient Copolymers. *J. Polym. Sci., Part B: Polym. Phys.* **2011**, *49*, 629.

(5) Mok, M.; Pujari, S.; Burghardt, W.; Dettmer, C.; Nguyen, S.; Ellison, C.; Torkelson, J. M. Microphase Separation and Shear Alignment of Gradient Copolymers. *Macromolecules* **2008**, *41*, 5818.

(6) Tito, N. B.; Milner, S. T.; Lipson, J. E. G. Self-Assembly of Lamellar Microphases in Linear Gradient Copolymer Melts. *Macromolecules* **2010**, *43*, 10612.

(7) Mok, M. M.; Ellison, C. J.; Torkelson, J. M. Effect of Gradient Sequencing on Copolymer Order Disorder Transitions: Phase Behavior of Styrene/n-Butyl Acrylate Block and Gradient Copolymers. *Macromolecules* **2011**, *44*, 6620.
(8) Mok, M. M.; Kim, J.; Wong, C.; Marrou, S.; Woo, D. J.; Dettmer, C. M.; Nguyen, S. T.; Ellison, C. J.; Shull, K. R.; Torkelson, J. M. *Macromolecules* **2009**, *42*, 7863.
(9) Mok, M. M.; Masser, K. A.; Runt, J.; Torkelson, J. M. Dielectric Relaxation Spectroscopy of Gradient Copolymers and Block Copolymers: Comparison of Breadths of Relaxation Time for Systems with Increasing Interphase. *Macromolecules* **2010**, *43*, 5740.
(10) Jiang, R.; Jin, Q.; Li, B.; Ding, D.; Wickham, R. A.; Shi, A. Phase Behavior of Gradient Copolymers. *Macromolecules* **2008**, *41*, 5457.
(11) Yuan, W.; Mok, M. M.; Kim, J.; Wong, C.; Marrou, S.; Woo, D. J.; Dettmer, C. M.; Nguyen, S. T.; Ellison, C. J.; Torkelson, J. M.; Shull, K. R. Behavior of Gradient Copolymers at Liquid/Liquid Interfaces. *Langmuir* **2010**, *26*, 3261.
(12) Ribaut, T.; Oberdisse, J.; Annighofer, B.; Fournel, B.; Sarrade, S.; Haller, H.; Lacroix-Desmazes, P. Solubility and Self-Assembly of Amphiphilic Gradient and Block Copolymers in Supercritical CO_2. *J. Phys. Chem. B* **2011**, *115*, 836.
(13) Mauri, M.; Thomann, Y.; Schneider, H.; Saalwachter, K. Spin-Diffusion NMR at Low Field for the Study of Multiphase Solids. *Solid State NMR* **2008**, *34*, 125.
(14) Thomann, Y.; Thomann, R.; Hasenhindl, A.; Mulhaupt, R.; Heck, B.; Knoll, K.; Steininger, H.; Saalwachter, K. Gradient Interfaces in SBS and SBS/PS Blends and Their Influence on Morphology Development and Material Properties. *Macromolecules* **2009**, *42*, 5684.
(15) Saalwachter, K. Proton Multiple-Quantum NMR for the Study of Chain Dynamics and Structural Constraints in Polymeric Soft Materials. *Prog. Nucl. Magn. Reson. Spectrosc.* **2007**, *51*, 1.
(16) Wang, X.; Coleman, J.; Jia, X.; White, J. L. Quantitative Investigations of Transient Acidity in Zeolites and Molecular Sieves. *J. Phys. Chem. B* **2002**, *106*, 4941−4946.
(17) (a) Spiess, H. W.; Schmidt-Rohr, K. *Multidimensional Solid-State NMR and Polymers*, 1994, Academic Press: San Diego, CA. (b) Mirau, P. A. *A Practical Guide to Understanding the NMR of Polymers*; Wiley and Sons: Hoboken, NJ, 2005.
(18) (a) Schmidt-Rohr, K.; Clauss, J.; Spiess, H. W. Correlation of Structure, Mobility, and Morphological Information in Heterogeneous Polymers by 2D Wideline Separation NMR Spectroscopy. *Macromolecules* **1992**, *25*, 3273−3277. (b) Spiess, H. W. Interplay of Structure and Dynamics in Macromolecular and Supramolecular Systems. *Macromolecules* **2010**, *43*, 5479−5491. (c) Gill, L.; Damron, J.; Wachowicz, M.; White, J. L. Glass Transitions, Segmental Dynamics, and Friction Coefficients for Individual Polymers in Multicomponent Polymer Systems by Chain Level Experiment. *Macromolecules* **2010**, *43*, 3903.
(19) Jouenne, S.; González-León, J. A.; Ruzette, A.; Lodefier, P.; Tencé-Girault, S.; Leibler, L. Styrene/Butadiene Gradient Block Copolymers: Molecular and Mesoscopic Structures. *Macromolecules* **2007**, *40*, 2432−2442.
(20) Litvinov, V. M.; Penning, J. P. *Macromol. Chem. Phys.* **2004**, *205*, 1721.
(21) White, J. L.; Beck, L. W.; Ferguson, D. B.; Haw, J. F. Background Suppression in Magic-Angle Spinning NMR. *J. Magn. Reson.* **1992**, *100*, 336−341.